

Multielectron dissociative ionization of O_2 in an intense picosecond laser field

D. Normand, C. Cornaggia, J. Lavancier, J. Morellec, and H. X. Liu
*Service de Physique des Atomes et des Surfaces, Centre d'Etudes Nucléaires de Saclay,
91191 Gif-sur-Yvette CEDEX, France*

(Received 22 October 1990; revised manuscript received 14 March 1991)

The multielectron dissociative ionization of O_2 has been studied using an intense picosecond laser at 610 and 305 nm in the 10^{13} – 10^{15} W/cm² laser intensity range. The excitation mechanisms producing multicharged dissociating molecular ions are determined from the kinetic energies and laser-intensity dependences of the atomic oxygen ions following the fragmentation of the molecule. Both at 305 and 610 nm, the multicharged atomic fragments (O^+ , O^{2+} , O^{3+} , O^{4+}) are produced from parent molecular ions that are sequentially ionized as they dissociate. Moreover, the transitions occur at well-defined internuclear distances independent of the peak laser intensity. A comparison with previous results obtained on N_2 and CO is discussed.

I. INTRODUCTION

The photodissociation of small molecular systems by intense laser fields (peak power up to 10^{16} W/cm²) is a subject of great interest both theoretical [1,2] and experimental [3-6]. The main result of the interaction process between the molecule and the laser radiation concerns the production of energetic fragments arising from multicharged parent molecular ions. Two ionization mechanisms have been invoked to account for the previous experimental findings. (i) Around 600 nm [6-9], the successive ionization steps progress in a nonvertical way, i.e., at increasing internuclear distances, and accompany the coulombic explosion of the molecule. The most striking aspect of the process is that the ejections of the electrons occur at fixed internuclear distances whatever the peak laser intensity. (ii) At 248 [3,10] and 305 nm [6,7], the experimental results indicate that the molecular ionizations arise at about the internuclear distance of the neutral molecule. Moreover, it appears that the charge asymmetric channels are favored at these wavelengths and that the interaction creates lower molecular charge states than at 600 nm.

The differences observed between the results of 305 and 610 nm on N_2 and CO have been interpreted as resulting from the population of nonidentical electronic states of the doubly charged molecule [6,7]. At 610 nm, the N_2^{2+} and CO^{2+} molecules dissociate before the extinction of the laser pulse and are thus susceptible to lose additional electrons during the fragmentation process. At 305 nm, the molecular states populated have longer dissociative lifetimes (greater than the laser pulse duration) which induces vertical excitations of the molecules. This interpretation implies that other molecules should show a different behavior, depending on the molecular states populated at 305 and 610 nm.

We report the study of the O_2 molecule when irradiated by an intense laser radiation (wavelength 305 and 610 nm; pulse duration 2 ps). To identify the detailed dynamics of the interaction process, we measure the kinetic en-

ergies of the dissociation products and study the ion yield dependences on the laser intensity in the range of 10^{13} – 5×10^{15} W/cm². The results are presented in Sec. III (610 nm) and Sec. IV (305 nm) after a short description of the experimental setup given in Sec. II. The conclusion is given in Sec. V.

II. EXPERIMENTAL SETUP

The experimental arrangement, including laser system, has already been described in detail elsewhere [6]. Briefly, the basic components of the experimental setup are the following. The pulses delivered by a synchro-pumped dye laser are amplified through a four-stage dye amplifier pumped by a Nd:YAG laser operating at 10 Hz. The output energy is about 3 mJ at 610 nm. Two different lenses have been alternatively used to focus the laser beam. The former is a spheroparabolic lens of 60 mm focal length that focuses the laser light on a near-diffraction-limited focal section of 2.2×10^{-7} cm² at 610 nm and 7.8×10^{-7} cm² at 305 nm. The latter has a focal length of 150 mm and focuses the laser beam on a spot section of 1.3×10^{-6} cm² at 610 nm.

The laser pulse duration after amplification is measured using second-harmonic generation and single-shot autocorrelation techniques. Assuming a Gaussian intensity profile, we have found a value of 2 ps. The 305-nm laser radiation is obtained after frequency doubling in a BBO crystal (conversion efficiency 15%) that shortens the laser pulse duration to 1.4 ps at this wavelength. The available maximum laser intensities are 5×10^{14} W/cm² at 305 nm and 5×10^{15} W/cm² at 610 nm.

The detection system consists in a double-chamber time-of-flight (TOF) ion mass spectrometer pumped at a background pressure of 10^{-9} Torr [11]. The application of a weak-collection electric field in the interaction chamber makes it possible to determine the fragment kinetic energies with good precision (10%) whereas the second chamber strongly accelerates the ions to ensure a good collection efficiency. Finally, the ions are mass

separated through an 18-cm-long drift tube and give a signal that feeds a Lecroy model 9400 transient digitizer with a 100-MHz sampling frequency.

III. STUDY AT 610 nm

A. Experimental results

The overall TOF spectrum arising from the multielectronic dissociative ionization of O_2 recorded at 4×10^{15} W/cm² is illustrated in Fig. 1. The strong-collection electric field (900 V/cm) gathers into a single peak the ions with the same ratio q/m (q and m being, respectively, the charge and mass of the ion) whatever their initial kinetic energies. Four charge states of the atomic oxygen, O^+ up to O^{4+} , and two classes of molecular ions, O_2^+ and O_2^{2+} , are produced during the interaction. The O^+ and O_2^+ ion species cannot be distinguished because of the high extraction field. The predominance of the O_2^+ peak indicates a rather low fragmentation rate even at 4×10^{15} W/cm². In the case of N_2 and CO , the dissociative channels were observed to be more important for O_2 at this laser intensity with the same pulse duration of 2 ps [6,7].

The kinetic energies of the atomic fragments are measured with a small extraction electric field ranging from 20 to 80 V/cm to ensure a good resolution. For each ion species, a double-peak structure can be seen in Fig. 2(a)–2(d) where the laser polarization lies along the axis of detection. The faster components represent ions initially ejected toward the detector while the slower components come from ions initially released in the opposite direction and whose momenta have been reversed by the extraction electric field. The kinetic energy is deduced from the simple formula

$$E = \frac{1}{8}(q^2/m)F^2\Delta t^2, \quad (1)$$

where F is the extraction electric field and Δt the

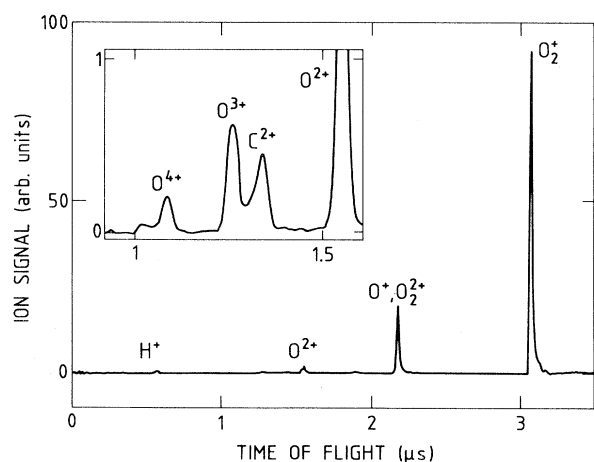


FIG. 1. TOF ion mass spectrum of O_2 produced at 610 nm and 4×10^{15} W/cm². The extraction field in the interaction chamber is 900 V/cm and the O_2 pressure is 1.5×10^{-8} Torr. The top left window is recorded with a $50 \times$ higher oscilloscope sensitivity to show the O^{3+} and O^{4+} ion peaks.

difference of time of flight between the “away” and “toward” components. The precision of the measurements is improved by recording the spectra for different extraction fields. The kinetic energies are then calculated according to Eq. (1), and averaged over the set of data. The experimental results obtained at 4×10^{15} W/cm² are gathered in Table I (the slow O^+ components can only be resolved at very low values of F). In order to avoid space-charge effects, the O_2 pressure during the experiments is kept low, in the range 10^{-8} – 10^{-6} Torr. We have shown elsewhere [6,7] that the kinetic energies of the atomic ions can be increased if the number of charges in the focal spot becomes too important.

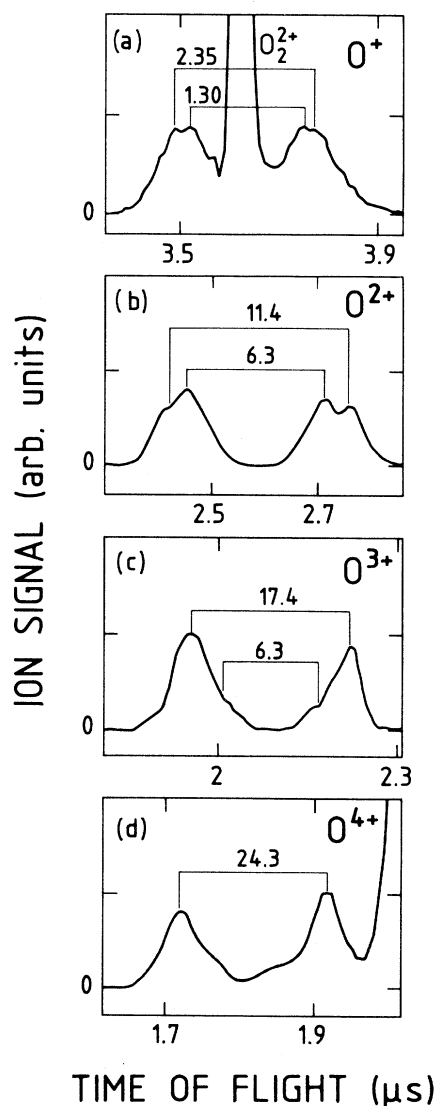


FIG. 2. TOF ion mass spectra of O_2 recorded at 610 nm and 4×10^{15} W/cm². The operating pressure is adjusted in order to maintain a constant ion yield. A small extraction field of 60 V/cm is applied in order to distinguish the different classes of velocities for each group of atomic ions: (a) O^+ and O_2^{2+} ions, (b) O_2^+ ions, (c) O^{3+} ions, (d) O^{4+} ions.

TABLE I. Initial kinetic energies and power laws of the main ion classes observed at 610 nm.

	Initial energy (eV)	Power law (K)
O ₂ ⁺	0	6.6±0.7
O ⁺	0.36±0.05	7.1±0.7
	0.68±0.10	
	1.30±0.15	
	2.35±0.25	
O ²⁺	6.3±0.7	8±0.8
	11.4±1.2	
O ³⁺	6.3±0.7	6±0.7
	17.4±1.8	
O ⁴⁺	24.3±2.5	

In addition to the initial kinetic-energy measurements, a complementary way to investigate the multielectronic ionization of molecules is to study the laser-intensity dependence of the atomic and molecular ion species (Fig. 3). As can be seen in Fig. 2(a), the application of a small extraction field, 60 V/cm, permits one to distinguish the O⁺ atomic ions from the O₂²⁺ molecular ions, and thus to measure separately their laser-intensity dependences. The curves of Fig. 3 exhibit a linear progression in log-log coordinates followed by a saturation as the laser intensity increases. The linear part is characterized by the power law $k = d\log_{10}(N_i)/d\log_{10}(I)$ where N_i is the number of ions and I the peak laser intensity (Table I). The saturation part is due to the depletion of the initial-state population responsible for the ion formation.

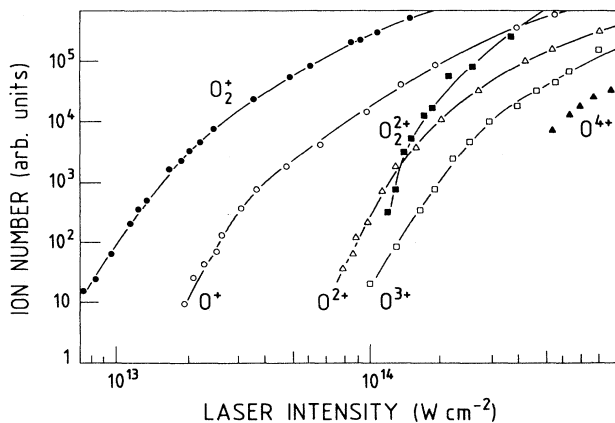


FIG. 3. Number of ions detected as a function of peak laser intensity at 610 nm.

B. Discussion

It is clear from Fig. 3 that the peak laser intensity is the key parameter governing the ionization degrees of the molecule. Below 2×10^{13} W/cm², we detect only O₂⁺ molecular ions. The measured power-law coefficient $k = 6.6 \pm 0.7$ is in close agreement with the fact that seven 610-nm photons are necessary to ionize the molecule to the O₂⁺ X ²Π_g ground state. Above 1.5×10^{13} W/cm², the O₂⁺ signal saturates due to the depletion of the O₂ ground-state population as the laser intensity continues to increase in the focal volume.

Up to 8×10^{13} W/cm², the laser-molecule interaction produces only O⁺ and O₂⁺ ions. It should be noted that Fig. 3 represents the intensity dependence of the total number of atomic ions, whatever their initial kinetic energy. The energy spectrum of the O⁺ ions at two different laser intensities can be seen in Fig. 4. At 5×10^{13} W/cm², the 0.36 and 0.68-eV ion species dominate the 1.30- and 2.35-eV ion classes while we observe the inverse behavior at 8×10^{14} W/cm². Thus, the increasing laser intensity favors the higher energies for a given atomic fragment. This general trend in our experiments has also been observed for CO [7], and at 305 nm for O₂ (see Sec. IV). The low-energy O⁺ ions are detected at a laser intensity above the saturation intensity (1.5×10^{13} W/cm²) of the O₂⁺ ions. This observation shows that these atomic ions are created after the molecular ions as the laser pulse rises. In particular, the dissociation of the neutral molecule followed by the ionization of the fragments would be simultaneous with the O₂⁺ production since this process is expected to have the same laser-intensity behavior as the multiphoton ionization of O₂. In addition, the O⁺ energies up to 1.3 eV are too small to come from a Coulombic O⁺+O⁺ channel that produces faster ions. As a conclusion, below 8×10^{13} W/cm², we observe the multiphoton dissociation of O₂⁺. At least four 610-nm photons are necessary to dissociate

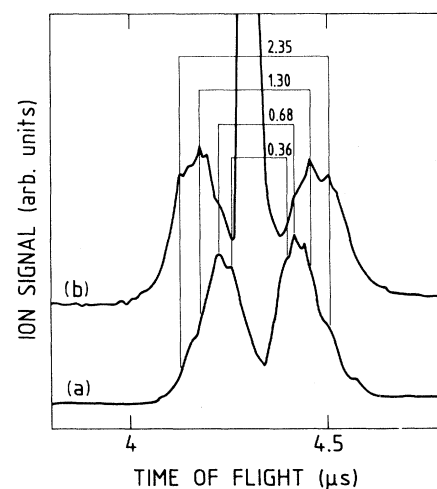
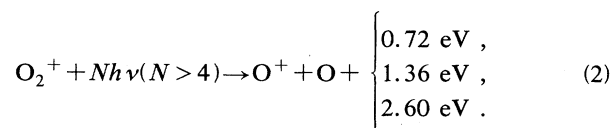


FIG. 4. TOF spectra of O⁺ ions recorded at 50 V/cm for two different laser intensities: (a) $I = 5 \times 10^{13}$ W/cm²; (b) $I = 8 \times 10^{14}$ W/cm².

the $O_2^+ X^2\Pi_g$ ground state according to



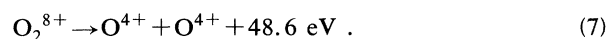
As the laser intensity is increased above 8×10^{13} W/cm², we detect O^{2+} , O^{3+} , O^{4+} atomic ions as well as O_2^{2+} molecular ions (Fig. 3). In addition, the 2.35-eV O^+ ion class becomes a major contribution of the O^+ TOF spectrum [Fig. 2(a) and Fig. 4]. The question is now to determine which of the following processes is responsible for this ion class:

- (i) $O_2^{2+} \rightarrow O^+ + O^+ + 4.7 \text{ eV}$,
- (ii) $O_2^+ \rightarrow O^+ + O + 4.7 \text{ eV}$,
- (iii) $O_2^{+*} \rightarrow O^+ + O^+ + 4.7 \text{ eV} + e^-$.

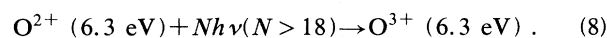
Case (i) can be eliminated for three reasons. (1) The threshold laser-intensity values corresponding to the detection of the 2.35-eV O^+ and O_2^{2+} ions are different: respectively 5.10^{13} [Fig. 4(a)] and 10^{14} W/cm². (2) The laser-intensity dependence of the O_2^{2+} ion number is steeper than the O^+ corresponding variation even in the saturated region where the 2.35-eV ions are predominant (Fig. 3). Case (i) would imply an O^+ laser-intensity dependence at least as steep as the O_2^{2+} one. Moreover, using the same argument, the production of O^{2+} , O^{3+} , and O^{4+} cannot be correlated to the O_2^{2+} ground state by subsequent multiphoton absorption from the molecular dication (Fig. 3). (3) The third reason comes from the electronic structure of O_2^{2+} [12,13]. In the case of a unimolecular fragmentation, the energy released in reaction (i) would imply the dissociation of a vibrational state situated very deep in the well of the $X^1\Sigma_g^+$ ground state of O_2^{2+} . Following the potential energy curve given by Larson *et al.*¹³, the tunneling from a low vibrational state of $X^1\Sigma_g^+$ to the $O^+ + O^+$ continuum is found to be unlikely.

We have now to distinguish between cases (ii) and (iii). Case (ii) is the same process as reaction (2) discussed above. The O_2^+ ion created by a multiphoton excitation from the O_2^+ ground state dissociates into a neutral atom and an ion. Case (iii) involves excited molecular states of the O_2^+ ion that autoionizes into the $O^+ + O^+$ continuum. The higher-appearance laser intensity of the 2.35-eV ion class compared with the laser intensity necessary to produce reaction (2) indicates that the physical origin of these ions takes place higher in the spectrum of the O_2^+ ion. As a conclusion, case (iii) is assumed to be the source of the 2.35-eV O^+ ions. The excited states involved in this process could be Rydberg states converging to the $X^1\Sigma_g^+$ electronic ground state of O_2^{2+} . However no assignment of such levels is possible within our experimental framework.

Taking into account the remaining O^{2+} , O^{3+} , and O^{4+} atomic ions, we propose the following sequence to explain the fragmentation dynamics at 610 nm above 8×10^{13} W/cm²:



In addition, we detect the subsequent ionization of the 6.3-eV O^+ ions following



In reactions (3)–(7) molecular ions are considered as transient species. Process (3) has been discussed in detail in the preceding paragraph. Processes (4) and (5) involve the 6.3 and 11.4 eV O^{2+} ion classes reported in Table I. There is still a non-negligible signal at 6.3 eV in the O^+ TOF spectrum and the height of the wings in Fig. 2(a) is comparable to the 6.3-eV O^{2+} signal if we take into account the scale factor due to the response of the electron multiplier cathode to different ion charge states. As a consequence, reaction (4) is assumed to occur as the transient dissociating ($O^+ + O^+$) complex is ionized by the laser field. Taking into account a Coulomb repulsive energy curve for the $O^+ + O^{2+}$ channel and the fact that the ($O^+ + O^+$) repulsion does not have any significant kinetic energy after the autoionization of O_2^{+*} , the ionization internuclear distance is estimated to be 2.3 Å. Similarly, reaction (5) happens after the creation of the $O^+ + O^{2+}$ fragmentation pathway and results from an ejection of an electron during the dissociation of this channel. Now both O_2^{3+} and O_2^{4+} transient molecular ions can be represented in first approximation by Coulomb repulsive energy curves and the resulting ionization internuclear distance is calculated to be 2.8 Å from the measured kinetic energies. Finally reactions (6) and (7) are quasiatomic ionization processes situated, respectively, at 6 and 7.3 Å. At such large internuclear distances, the laser-molecule interaction is more characterized by the simultaneous ionization of two mutually repelling fragments than by a two-electron ejection from a molecular ion. The sequential dynamics of the whole fragmentation pattern at 610 nm is illustrated in Fig. 5.

The most striking feature of our ion spectra is the independence of the energy of the fragments (issued from a given dissociative path) on the peak laser intensity. Indeed, in our interpretation, the successive ionization steps of the transient molecular ion takes place during its dissociation. The transitions occur between repulsive Coulombic states whose energy separation is R dependent: as R is decreased, the energy gap to jump over to extract and additional electron is increased. Therefore we expected that for higher laser intensities, a given ionization step (for instance $O_2^{3+} \rightarrow O_2^{4+}$) could occur at shorter internuclear distances (with a larger number of photons absorbed) leading to more energetic fragments. This expectation is contradicted by the following observation: the ionization of the dissociating molecular ions occur at fixed internuclear distance whatever the peak laser intensity. This still unexplained phenomenon has

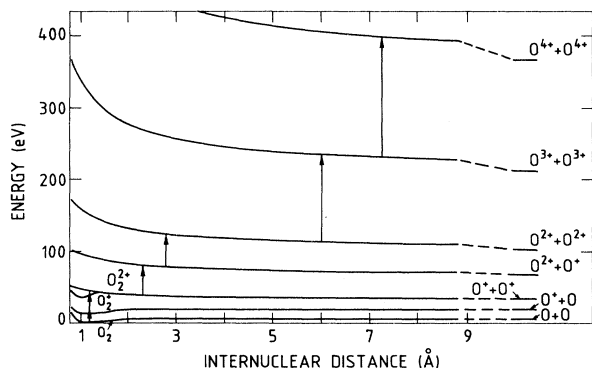


FIG. 5. Simplified potential-energy diagram of O₂ showing the ionization and dissociation events occurring at 610 nm. From O₂³⁺ the molecular coupling is described by the Coulombic repulsion between the two atomic fragments.

been observed in similar experiments with N₂ [6] and CO [7], and confirmed by covariance mapping techniques [8] with the same gases. We propose the following picture: during the rise time of the laser pulse, all the intensities are available up to the peak laser intensity, then each ionization channel picks up the necessary intensity to occur.

However this picture does not explain all the experimental findings. Indeed, since an ionization step occurs when a certain threshold intensity is reached within the rise time of the laser pulse, the energy of the fragments should depend on the pulse shape. This is denied by different experimental results.

(i) First, when the laser intensity is varied by a large amount, the threshold intensities are reached more or less rapidly (which means that the molecular ions “see” different pulse shapes), and yet the ionic fragment energies are unchanged.

(ii) In addition, we are repeating the MEDI experiments on O₂ with 100-fs laser pulses and the preliminary results yield the same fragment energies as with 2-ps pulses.

(iii) Finally, MEDI experiments have also been performed on N₂ and CO with laser pulse durations of 600 fs [5,8] and [6,7]. In the two cases the fragment energies measured were identical.

In conclusion, the multicharged molecular ion states are probably not simple Coulombic states. It may be that the dissociation of the molecular ions is slowed down by some screening effects due to the electrons. So far, this is still an open question.

IV. STUDY AT 305 nm

A. Experimental results

The interaction of O₂ molecules with a 305-nm laser radiation (peak power 3×10^{14} W/cm²) leads to the TOF ion mass spectrum represented on Fig. 6. We note that the fragmentation rate into O⁺ ions is higher than at 610 nm, which confirms the tendency already observed in the case of N₂ [6] and CO [7]. We detect three charge states

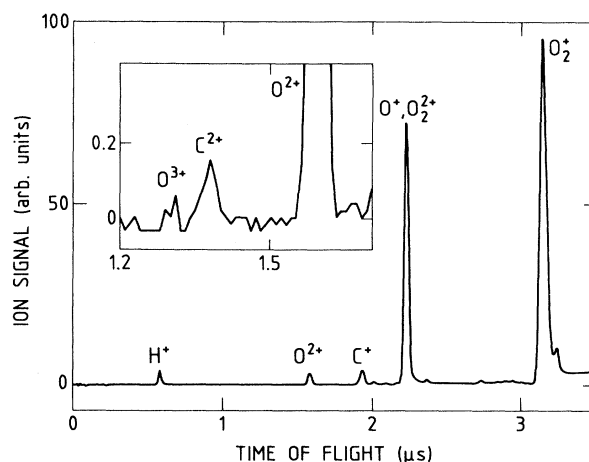


FIG. 6. TOF ion mass spectrum of O₂ obtained at 305 nm and 3×10^{14} W/cm². A 900-V high voltage is applied along the 10-mm interaction chamber and the pressure is 3×10^{-7} Torr.

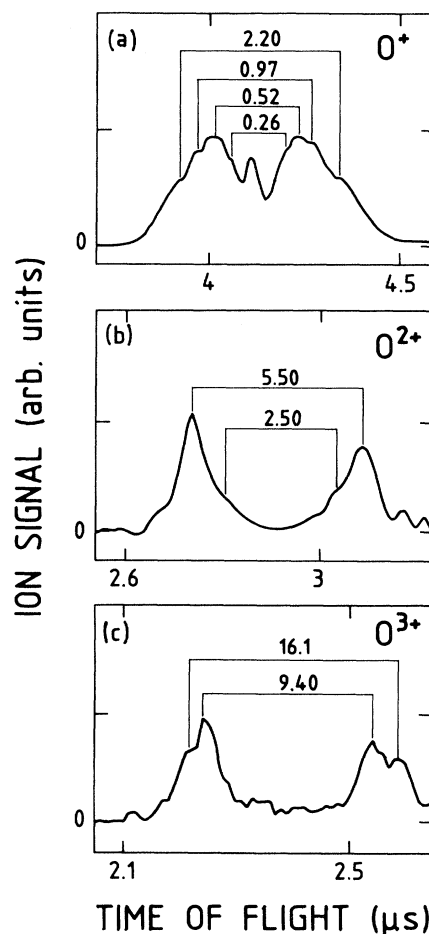


FIG. 7. TOF ion mass spectra of O₂ recorded at 305 nm and 3×10^{14} W/cm². The extraction field is 40 V/cm: (a) O⁺ ions, (b) O₂²⁺ ions, (c) O₂³⁺ ions.

TABLE II. Initial kinetic energies and power laws of the main ion classes observed at 305 nm.

	Initial energy (eV)	Power law (K)
O_2^+	0	1.5 ± 0.1
O^+	0.26 ± 0.03	3.7 ± 0.23
	0.52 ± 0.05	
	0.97 ± 0.10	
	2.20 ± 0.25	
O^{2+}	2.50 ± 0.30	6.2 ± 0.5
	5.50 ± 0.60	
O^{3+}	9.4 ± 1.0	
	16.1 ± 1.7	

of atomic fragments (O^+ , O^{2+} , and O^{3+}) and two classes of molecular ions (O_2^+ and O_2^{2+}). It is worth noting that no trication had been observed in the TOF spectrum of N_2 and CO at 305 nm.

As at 610 nm, the initial kinetic energies of the different ionic fragments are measured by applying weak-extraction electric fields in the interaction chamber [Fig. 7(a)–7(c)]. We note that an important contribution

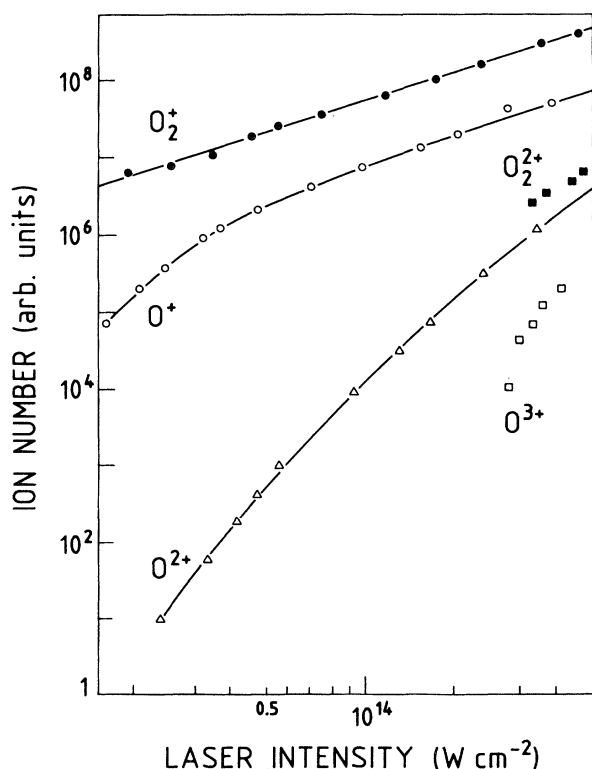


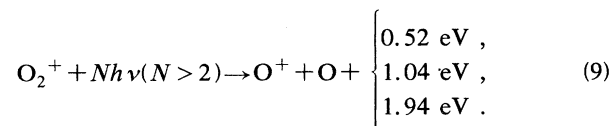
FIG. 8. Number of ions detected as a function of peak laser intensity at 305 nm.

of slow components is present in the O^+ ion peaks. Finally we have also measured the ion abundances as a function of the laser intensity in the range of 10^{13} to 5×10^{14} W/cm^2 . The experimental results (power laws and initial kinetic energies of the ions) are summarized in Table II.

B. Discussion

As can be seen in Fig. 8, the O_2^+ signal strongly dominates at low intensity (10^{13} W/cm^2) and saturates over the entire intensity range investigated (power law of 1.5 [14]). The ionization potential of O_2 is reached by absorption of at least three photons at 305 nm.

The fragmentation rate of molecular oxygen into O^+ ions increases with the laser intensity to reach 10% at 4×10^{13} W/cm^2 . Taken into account the initial kinetic energies of the slower O^+ fragments [Fig. 7(a)], three dissociative channels can unambiguously be attributed to the multiphoton dissociation of O_2^+ into the $O+O^+$ ion pair:



It must be pointed out that the preponderance of the O_2^+ population at low intensity implies that the O^+ ions cannot proceed from the multiphoton ionization of neutral fragments arising from the dissociation of O_2 . The fragmentation mechanism thus occurs after the O_2^+ formation.

At higher intensity (5×10^{14} W/cm^2), higher charge states of atomic and molecular ions have appeared in the TOF ion mass spectrum of O_2 . Considering the energies of the different ionic species detected (Table II), we suggest the following sequence of events at 305 nm:

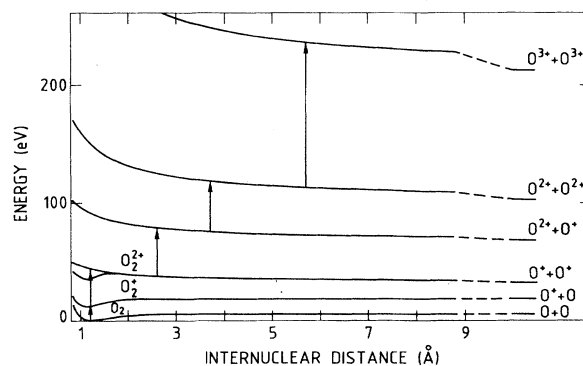
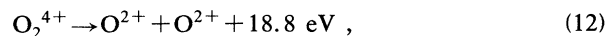


FIG. 9. Simplified potential-energy diagram of O_2 showing the ionization and dissociation events occurring at 305 nm.

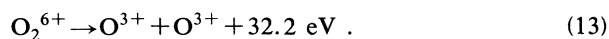
TABLE III. Kinetic energy (eV) released by the dissociation of multicharged N₂, O₂, and CO molecules. We have only indicated the cases where the ionization process has been found to be nonvertical. *R* denotes the mean internuclear distance at which the ionization occurs.

Dissociated channels	Molecule			CO	Mean energy	<i>R</i> (Å)
	N ₂	O ₂				
		305 nm	610 nm			
$AB^{3+} \rightarrow A^{+} + B^{2+}$	12	11	13	10 ^a /11 ^b	12±1	2.4
$AB^{4+} \rightarrow A^{2+} + B^{2+}$	20	19	23	19	21±2	3.2
$AB^{6+} \rightarrow A^{3+} + B^{3+}$	28	32	35	31 ^c	32±3	6.5

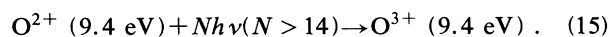
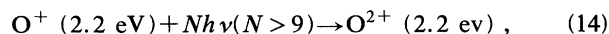
^aCO³⁺ → C²⁺ + O⁺.

^bCO³⁺ → C⁺ + O²⁺.

^cRef. 15.



The observation of the 5.5-eV O⁺ and 9.4-eV O²⁺ ions is difficult due to their weak abundances. Consequently these components only appear as small shoulders in their respective peaks. In reactions (10) and (13) occurring during the application of the laser pulse, we expect to observe subsequent ionization of the fragments. Indeed, we detect two classes of ions which are interpreted to be generated according to



Except for small differences concerning the initial kinetic energies of the fragments, the reactions occurring at 305 nm are almost identical to those observed at 610 nm (Fig. 9). In particular, the kinetic energy released in reactions (3) and (10) indicates that the electronic state of O₂⁺* populated during the interaction process is likely to be the same at 305 and 610 nm. The dissociation of this state initiating the whole sequence of events, it is not surprising to find similarities at both wavelengths. The nonobservation of O⁴⁺ ions is then simply related to the maximum laser intensity available, which is lower at 305 nm. As at 610 nm, we note that the population of metastable states of O₂²⁺* also occurs after the formation of O²⁺ ions. However, the formation of these molecular ions involves a higher laser intensity at 305 nm.

As a conclusion, the multiple ionizations of O₂ at 305 and 610 nm progress in a nonvertical way that is at increasing internuclear distances. This important result demonstrates that the laser wavelength does not govern directly the molecular response to the strong field.

V. CONCLUSION

The multiple ionization of O₂ progresses via nonvertical transitions both at 305 and 610 nm. This observation, which is the key point of the paper, demonstrates that the

laser wavelength does not have a direct influence on the dynamics of the process. Our experimental results indicate precisely the real role of the laser wavelength in the molecule radiation interaction process. Indeed, the comparison between these new results and the previous ones obtained on N₂ [6] and CO [7] in the same experimental conditions leads us to the following conclusions.

At 610 nm, all data show that the ionization processes are characterized by a nonvertical progression. Up to the double ionization, the ion energies differ according to the molecule that underlines the importance of the molecular structure in the first stages of the molecule-laser radiation interaction process. From the triple ionization process, the ion energies from a given dissociation channel are almost the same, whatever the molecule (Table III), confirming that the molecular coupling is then described by the Coulombic interaction between the two ionic fragments. It appears that the successive ionizations into AB³⁺, AB⁴⁺, and AB⁶⁺ occurs at fixed internuclear distances: respectively, 2.4, 3.2, and 6.5 Å.

At 305 nm, our findings for the O₂ are in sharp contrast with the previous results obtained on N₂ and CO where the transitions occur at about the equilibrium internuclear distance of the neutral molecule. In these later cases, the last step of the interaction is the population of high excited states of the molecular dication which dissociate into charge asymmetric fragments (e.g., CO²⁺* → C + O²⁺). The nonvertical progression observed in O₂ facilitates the formation of higher-charge states since the transient molecular ion O₂⁶⁺ appears in the sequence of events. To interpret our results, the key parameter concerns the population of the doubly charged molecular ion states (or autoionizing states of the single charge ion) whose dissociative lifetimes govern the orientation of the entire process. At 305 nm, we assume that the lifetimes of the populated states of CO²⁺ and N₂²⁺ are too long (compared to the laser-pulse duration) to allow the ignition of the stepwise Coulomb explosion processes observed on O₂.

- [1] K. Codling, L. J. Frasinski, and P. A. Hatherly, *J. Phys. B* **22**, L321 (1989).
- [2] M. Brewczyk and L. J. Frasinski (unpublished).
- [3] K. Boyer, T. S. Luk, J. C. Solem, and C. K. Rhodes, *Phys. Rev. A* **39**, 1186 (1989).
- [4] P. A. Hatherly, L. J. Frasinski, K. Codling, A. J. Langley, and W. Shaikh, *J. Phys. B* **23**, L291 (1990).
- [5] K. Codling, L. J. Frasinski, P. A. Hatherly and M. Stankiewicz, *Phys. Scr.* **41**, 433 (1990).
- [6] C. Cornaggia, J. Lavancier, D. Normand, J. Morellec, and H. X. Liu, *Phys. Rev. A* **42**, 5464 (1990).
- [7] J. Lavancier, D. Normand, C. Cornaggia, J. Morellec, and H. X. Liu, *Phys. Rev. A* **43**, 1 (1991).
- [8] L. J. Frasinski, K. Codling, and P. A. Hatherly, *Phys. Lett. A* **142**, 499 (1989).
- [9] K. Codling, L. J. Frasinski, P. Hatherly, and J. Barr, *J. Phys. B* **20**, L525 (1987).
- [10] G. Gibson, T. S. Luk, A. McPherson, K. Boyer, and C. K. Rhodes, *Phys. Rev. A* **40**, 2378 (1989).
- [11] W. C. Wiley and I. H. McLaren, *Rev. Sci. Instrum.* **26**, 1150 (1955).
- [12] N. H. F. Beebe, E. W. Thulstrup, and A. Andersen, *J. Chem. Phys.* **64**, 2080 (1976).
- [13] M. Larsson, P. Baltzer, S. Svensson, B. Wannberg, N. Martensson, A. Naves de Brito, N. Correia, M. P. Keane, M. Carlsson-Gothe, and L. Karlsson, *J. Phys. B* **23**, 1175 (1990).
- [14] S. L. Chin and N. R. Isenor, *Can. J. Phys.* **48**, 1445 (1970).
- [15] C. Cornaggia, J. Lavancier, D. Normand, and J. Morellec (unpublished).